

Article

Bio-Oriented Synthesis and Molecular Docking Studies of 1,2,4-Triazole Based Derivatives as Potential Anti-Cancer Agents against HepG2 Cell Line

Naheed Akhter ¹, Sidra Batool ², Samreen Gul Khan ^{2,*}, Nasir Rasool ², Fozia Anjum ², Azhar Rasul ³ , Şevki Adem ⁴, Sadaf Mahmood ², Aziz ur Rehman ⁵, Mehr un Nisa ⁶, Zainib Razzaq ², Jørn B. Christensen ⁷ , Mohammed A. S. Abourehab ⁸ , Syed Adnan Ali Shah ^{9,10,*}  and Syahrul Imran ^{10,11} 

- ¹ Department of Biochemistry, Faculty of Life Science, Government College University Faisalabad, Faisalabad 38000, Pakistan
 - ² Department of Chemistry, Drug Design and Medicinal Chemistry Laboratory, Faculty of Physical Science, Government College University, Faisalabad 38000, Pakistan
 - ³ Department of Zoology, Faculty of Life Sciences, Government College University Faisalabad, Faisalabad 38000, Pakistan
 - ⁴ Department of Chemistry, Faculty of Sciences, Çankırı Karatekin University, 18100 Çankırı, Turkey
 - ⁵ Department of Chemistry, Government College University, Lahore 54000, Pakistan
 - ⁶ Department of Chemistry, University of Lahore, Lahore 40100, Pakistan
 - ⁷ Department of Chemistry, Faculty of Science, University of Copenhagen, 2100 Copenhagen, Denmark
 - ⁸ Department of Pharmaceutics College of Pharmacy, Umm Al-Qura University, Makkah 21955, Saudi Arabia
 - ⁹ Faculty of Pharmacy, Universiti Teknologi MARA Cawangan Selangor Kampus Puncak Alam, Bandar Puncak Alam 42300, Selangor D. E., Malaysia
 - ¹⁰ Atta-ur-Rahman Institute for Natural Product Discovery (AuRIns), Universiti Teknologi MARA Cawangan Selangor Kampus Puncak Alam, Bandar Puncak Alam 42300, Selangor D. E., Malaysia
 - ¹¹ Faculty of Applied Sciences, Universiti Teknologi MARA Shah Alam, Shah Alam 40450, Selangor D. E., Malaysia
- * Correspondence: samreengul@gcuf.edu (S.G.K.); syedadnan@uitm.edu.my (S.A.A.S.); Tel.: +92-300-427-0077 (S.G.K.); +60-3-3258-4616 or +60-19365-1307 (S.A.A.S.)



Citation: Akhter, N.; Batool, S.; Khan, S.G.; Rasool, N.; Anjum, F.; Rasul, A.; Adem, Ş.; Mahmood, S.; Rehman, A.u.; Nisa, M.u.; et al. Bio-Oriented Synthesis and Molecular Docking Studies of 1,2,4-Triazole Based Derivatives as Potential Anti-Cancer Agents against HepG2 Cell Line. *Pharmaceuticals* **2023**, *16*, 211. <https://doi.org/10.3390/ph16020211>

Academic Editors: Valentina Noemi Madia, Michael Schmiech and Antonella Messori

Received: 5 December 2022

Revised: 20 January 2023

Accepted: 23 January 2023

Published: 30 January 2023



Copyright: © 2023 by the authors. Licensee MDPI, Basel, Switzerland. This article is an open access article distributed under the terms and conditions of the Creative Commons Attribution (CC BY) license (<https://creativecommons.org/licenses/by/4.0/>).

Abstract: Triazole-based acetamides serve as important scaffolds for various pharmacologically active drugs. In the present work, structural hybrids of 1,2,4-triazole and acetamides were furnished by chemically modifying 2-(4-isobutylphenyl) propanoic acid (**1**). Target compounds **7a–f** were produced in considerable yields (70–76%) by coupling the triazole of compound **1** with different electrophiles under different reaction conditions. These triazole-coupled acetamide derivatives were verified by physicochemical and spectroscopic (HRMS, FTIR, ¹³CNMR, and ¹HNMR,) methods. The anti-liver carcinoma effects of all of the derivatives against a HepG2 cell line were investigated. Compound **7f**, with two methyl moieties at the ortho-position, exhibited the highest anti-proliferative activity among all of the compounds with an IC₅₀ value of 16.782 µg/mL. **7f**, the most effective anti-cancer molecule, also had a very low toxicity of 1.190.02%. Molecular docking demonstrates that all of the compounds, especially **7f**, have exhibited excellent binding affinities of –176.749 kcal/mol and –170.066 kcal/mol to c-kit tyrosine kinase and protein kinase B, respectively. Compound **7f** is recognized as the most suitable drug pharmacophore for the treatment of hepatocellular carcinoma.

Keywords: 2-(4-isobutylphenyl) propanoic acid; hepatocellular carcinoma; anti-cancer; 1,2,4-triazole; molecular docking; acetamides

1. Introduction

In the 21st century, cancer and other infectious diseases are the most prevalent causes of death globally [1]. According to the World Health Organization (WHO), 11.5 million deaths are expected by 2030 due to cancer [2]. Among all types of cancer, hepatocellular carcinoma is among the leading causes of death, accounting for approximately 92% mortality rates

worldwide [3,4]. Thus, the development of new anti-cancer drugs remains a huge clinical need for improving therapeutic efficacy and controlling cancer [5]. The development of multi-target anti-cancer agents is the major focus of researchers globally due to the different drawbacks associated with already-used chemotherapeutics such as undesirable side effects, a lack of selectivity, systemic toxicity, and the emergence of multidrug resistance [6–9]. Intensive efforts must be made to discover and develop new, effective, tailored –anti-cancer agents with better safety profiles and drug-like properties.

Structurally modified nitrogen-containing heterocyclic moieties have a broad spectrum of applications for the development of novel therapeutic drugs as shown in Figure 1 [10,11]. Approximately 75% of Food and Drug Administration-approved drugs are nitrogen-based moieties [12]. Nitrogen-containing heterocyclic compounds have been synthesised in large numbers in recent times. They exhibit anti-tubercular [13], anti-cancer [14], anti-fungal [15], anti-microbial [16], anti-viral [17], and other biological properties such as genotoxicity and lipid peroxidation [18], and anti-inflammatory properties [19].

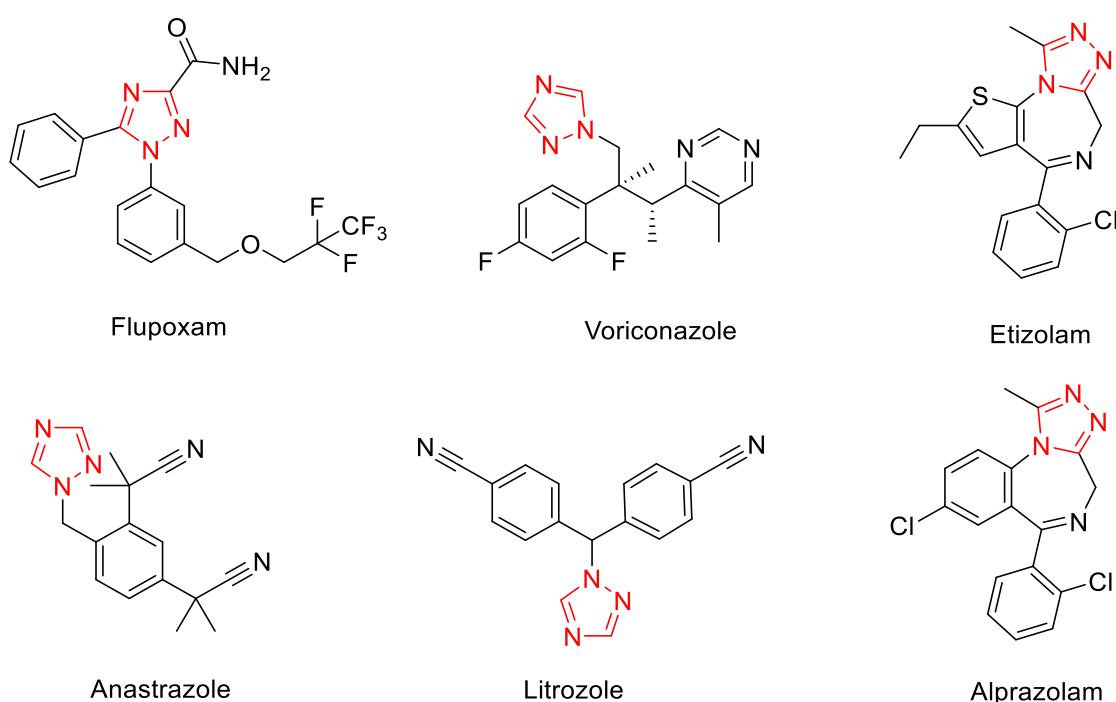


Figure 1. Structure of some common 1,2,4-triazole-based drugs.

Molecular hybridization is an easy and efficient method to combine various important drug pharmacophores. Our ongoing research focuses on the design and synthesis of pharmacologically active, diverse polyvalent scaffolds as anti-cancer agents. The versatile nature of 1,2,4-triazole has been reported to be of great importance in medicinal chemistry, such as for its anti-cancer [20], anti-fungal [21], anti-bacterial [22], anti-microbial, and anti-tumor properties [23], as well as pyrophosphatases and phosphodiesterase [24]. Acetamide has been identified as the most significant pharmacophore of anti-cancer drugs [25].

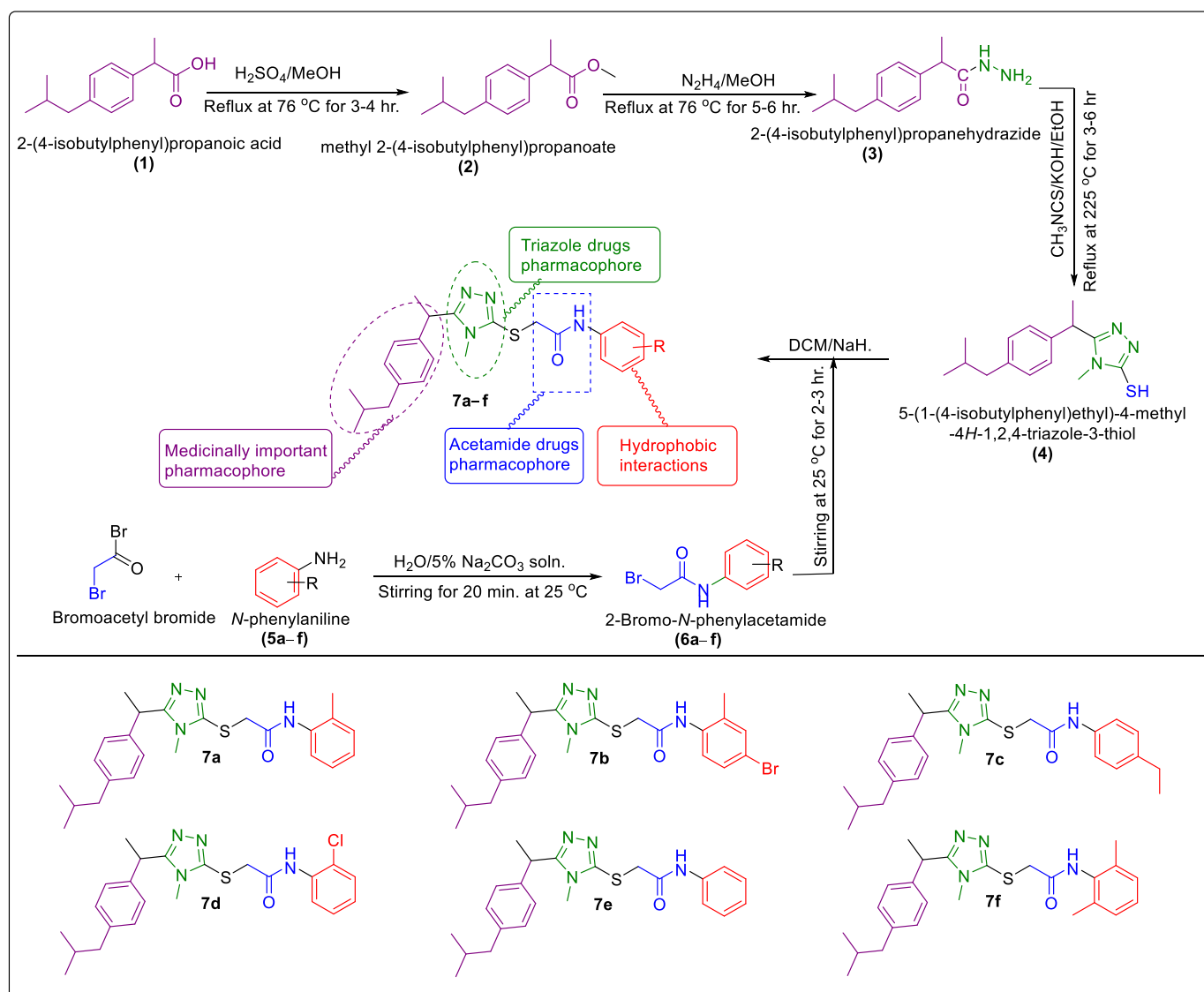
On this basis, we have created a hybrid of acetamide and 1,2,4-triazole pharmacophore by chemical derivatization of 2-(4-isobutylphenyl)propanoic acid in an attempt to avoid tumor progression. On each side of triazole and acetamide, we developed a molecular framework with hydrophobic aryl rings. It improves the solubility of the drug and its candidacy as a good drug molecule. Earlier, we reported the synthesis of various structural hybrids of oxadiazole-based acetamide [26–29], and it has been proven from the literature that heterocycle-based compounds possess good anti-cancer activity [30]. Thus, in an extension of our earlier research on heterocycles, –COOH group of 2-(4-isobutylphenyl)propanoic acid was cyclized into a 1,2,4-triazole ring 4.

2. Results

2.1. Chemistry

In the current study, 2-(4-isobutylphenyl)propanoic acid has been chemically modified with improved clinical utility. Different *N*-arylated 5-aryl-1,2,4-triazole-coupled acetamides (**7a–f**) have been synthesized in good yields by replacement of the H group of SH with various electrophiles.

Scheme 1 depicts the synthetic route of final compounds **7a–f**. The Fischer esterification method was used to create compound **2** by refluxing compound **1** with absolute CH₃OH at 76 °C for 3–4 h [31,32]. Compound **2** was slowly refluxed at 76 °C for 3–4 h with hydrazine hydrate [32] in CH₃OH and yielded 2-(4-isobutylphenyl)propane hydrazide (**3**). Molecule **3** was converted into its respective 5-(1-(4-isobutylphenyl) ethyl)-1,2,4-triazole-2-thiol (**4**) by slowly heating it at 225 °C for 3–6 h with methyl isothiocyanate in 10% NaOH and absolute CH₃OH. Upon completion, the reaction was acidified to pH 4–5 with conc. HCl. Upon acidification, precipitates appeared that had been separated as compound **4** by the process of filtration. At room temperature, compound **4** was treated with various *N*-arylated aralkyl/alkyl/aryl 2-bromoacetamides (**6a–f**) along with DCM and NaH as catalysts. The structures of triazole-coupled acetamide scaffolds were verified by physiochemical and spectroscopic (HRMS, FTIR, ¹³CNMR, and ¹HNMR) methods.



Scheme 1. Synthesis of 1,2,4-triazole-cored acetamides **7a–f**.

In the ^1H NMR spectrum, $-\text{NH}$ protons of the acetamide were the most deshielded and their chemical shift value was observed around 10.27–9.64 ppm. In propanoic acid, the protons of the aliphatic region were among the most shielded, with values ranging from 0.86–0.84 ppm. The presence of acetamide was confirmed by the appearance of signals around 4.04 ppm for the CH_2 group and in the range of 10.27–9.64 ppm for the NH group. In ^{13}C NMR, the appearance of $\text{C}=\text{O}$ signals in the range of 164.15–168 ppm confirmed the synthesis of acetamide. The presence of a triazole ring in the final derivatives was also confirmed by the appearance of signals in the range of 158.15 ppm and at 29.58 ppm for $\text{N}-\text{CH}_3$. In the ^1H NMR spectrum, signals for $\text{N}-\text{CH}_3$ were observed around 3.28 ppm. A distinctive peak around 22.0 ppm corresponded to the protons of two $-\text{CH}_3$ carbon nuclei. Signals for the CH_2 groups were observed between 44.18 to 20.19 ppm. By introducing some electron-withdrawing substitutions and comparing them to electron-donating group substitutions, we reported structure–activity relationships for the phenyl group. 3,5-disubstituted triazole nuclei have a versatile nature and are important in the pharmaceutical industry. On the basis of their medicinal importance, the anti-cancer activities of all of the compounds were checked.

2.2. Anti-proliferative Potential

The anti-hepatocellular activity of afforded *N*-arylated 1,2,4-triazole coupled acetamides (**7a–f**) was evaluated via MTT assay and these structural hybrids were screened against a liver cancer HepG2 cell line [33]. All of the compounds demonstrated mild to outstanding anti-cancer activity, as shown in Table 1. Among all of the compounds, **7f**, with two methyl groups at positions 2 and 6 of the phenyl ring, displayed the best anti-cancer potential with $\text{IC}_{50} = 16.782 \mu\text{g}/\text{mL}$. Compound **7a**, which contains a methyl at position 2 of the phenyl ring, also displayed good anti-cancer activity with an IC_{50} value of $20.667 \mu\text{g}/\text{mL}$ but less than **7f**. Compounds **7b**, **7c**, and **7e** also exhibited a significant anti-cancer effect but less than **7f** and **7a**. Compound **7d**, with an electron-withdrawing Cl substituent, displayed the lowest anti-hepatocellular activity with a $39.667 \mu\text{g}/\text{mL}$ IC_{50} value.

Table 1. The anti-hepatocellular carcinoma and hemolytic activities of triazole-coupled acetamides **7a–f**.

Compound	Alkyl/Aryl	Cell Viability IC_{50} Value ($\mu\text{g}/\text{mL}$)	Hemolytic Activity (Mean% \pm S.D)
7a	2-methyl phenyl	20.667	2.46 ± 0.31
7b	2-methyl-4-bromo phenyl	33.565	2.43 ± 0.11
7c	4-ethyl phenyl	39.002	4.32 ± 0.24
7d	2-chloro phenyl	39.667	7.33 ± 0.42
7e	phenyl	39.105	4.19 ± 0.02
7f	2,6-dimethyl phenyl	16.782	1.19 ± 0.02
Sorafenib		05.971	
PBS			0.00 ± 0.0
Triton-X-100			100 ± 0.0

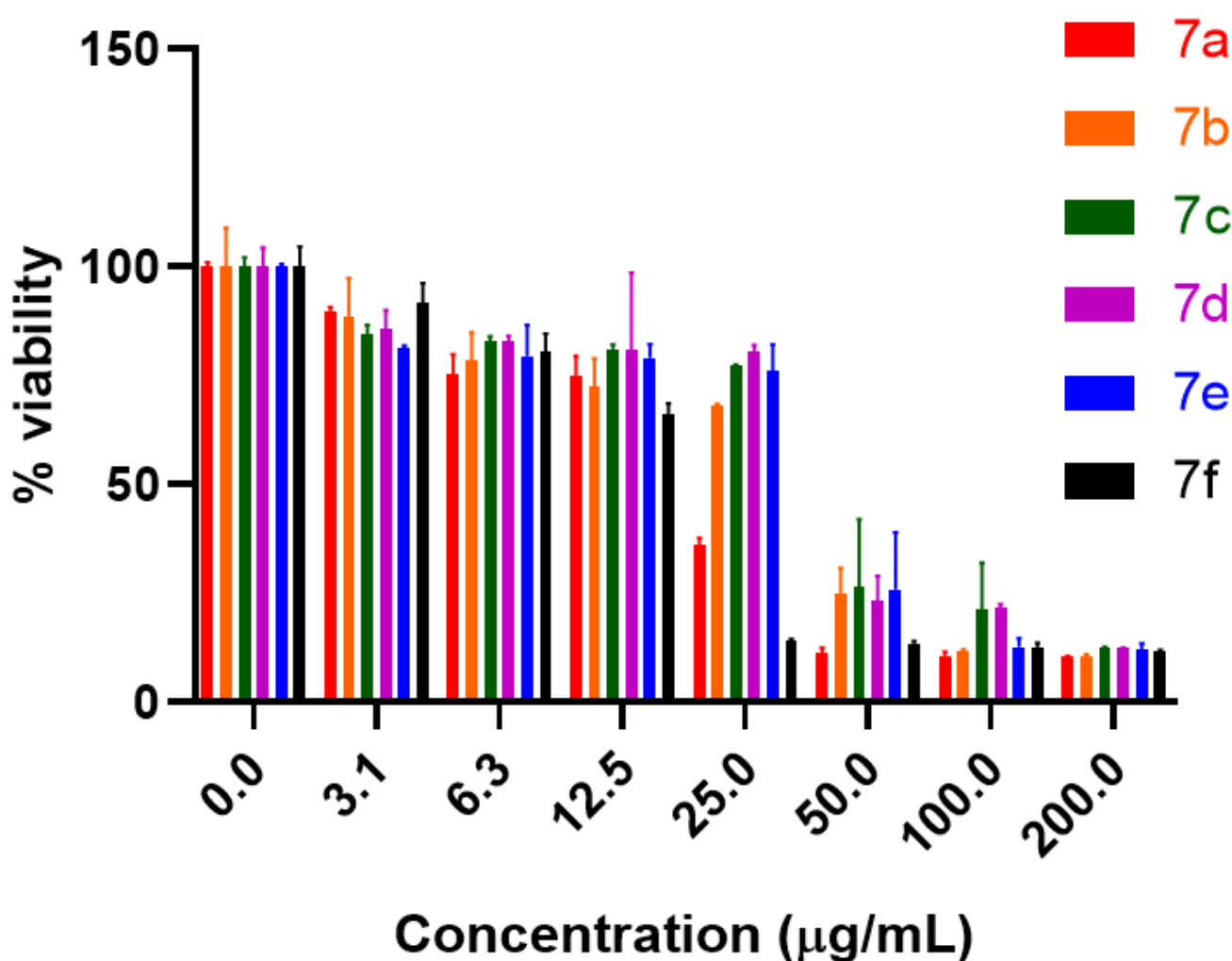
The cell viability of all of the compounds was further evaluated using various concentrations (3.125–200 μg) to test the dose response and % inhibition relationship as shown in Table 2.

Figure 2 shows that compounds **7f** and **7a** produced the best results at a 25 $\mu\text{g}/\text{mL}$ dose among all of the compounds.

The dose response and % inhibition of the most potent compound, **7f**, was checked at various concentrations (Figure 3).

Table 2. % inhibition of derivatives 7a–f at different concentrations ($\mu\text{g/mL}$).

Concentration ($\mu\text{g/mL}$)	7a	7b	7c	7d	7e	7f
200	89.40 \pm 0.34	89.50 \pm 0.06	87.51 \pm 0.20	87.70 \pm 0.18	88.00 \pm 1.44	88.36 \pm 0.31
100	88.17 \pm 0.26	89.39 \pm 0.91	78.82 \pm 10.78	78.33 \pm 0.78	87.34 \pm 2.09	87.71 \pm 1.34
50	75.18 \pm 5.99	88.64 \pm 1.11	73.66 \pm 15.54	76.69 \pm 5.63	74.24 \pm 13.16	86.57 \pm 0.56
25	63.98 \pm 1.67	31.90 \pm 0.30	22.82 \pm 0.29	19.52 \pm 1.44	24.01 \pm 6.12	85.90 \pm 0.30
12.5	27.70 \pm 6.46	25.23 \pm 4.67	19.14 \pm 1.25	19.11 \pm 17.71	20.99 \pm 3.13	33.96 \pm 2.47
6.25	21.44 \pm 6.24	24.75 \pm 4.62	17.35 \pm 1.32	17.32 \pm 1.40	20.52 \pm 7.11	19.55 \pm 4.07
3.125	11.57 \pm 8.85	10.33 \pm 0.96	15.40 \pm 2.01	14.27 \pm 4.27	18.65 \pm 0.50	8.40 \pm 4.54
DMSO (-ve Control)	0.0	0.0	0.0	0.0	0.0	0.0

**Figure 2.** Dose response and % cell viability of compounds 7a–f at different concentrations.

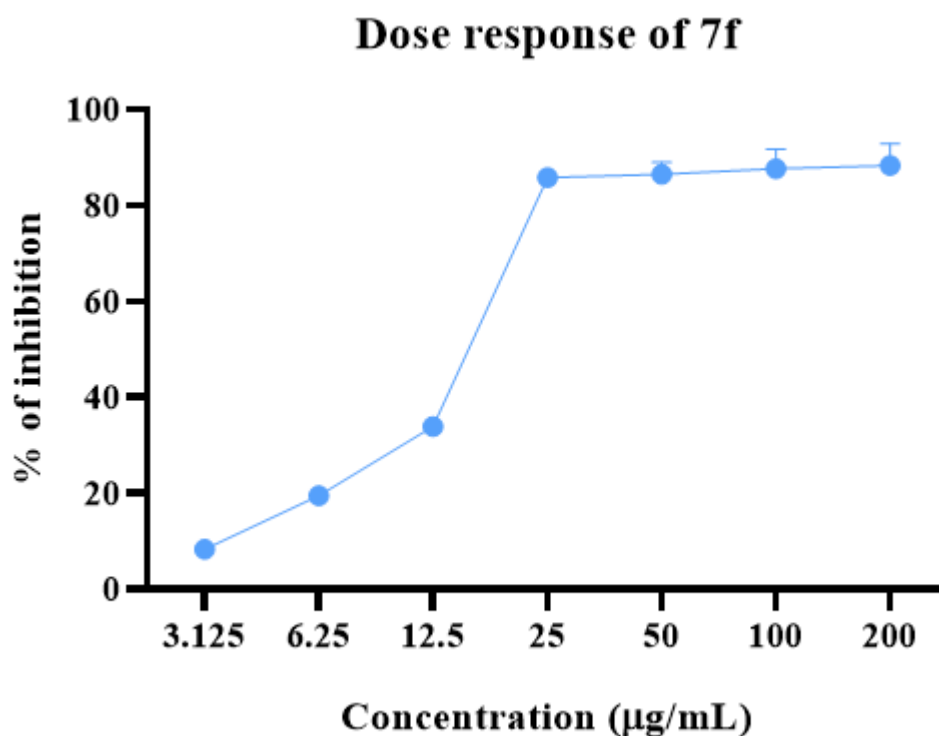


Figure 3. Dose response and % inhibition relationship of compound 7f at different concentrations.

2.3. Hemolytic Activity Potential

Hemolytic activity was investigated by the reported method [34] using Triton-X-100 as a standard. All of the triazole-based acetamide derivatives showed very low cytotoxicity, as shown in Table 1. Molecule 7f also presented very low toxicity at 1.19 ± 0.02 relative to reference Triton-X-100. All of the other compounds had moderately good hemolytic activity. Compounds 7a (2.46%), 7b (4.43%), 7c (4.32%), 7e (4.19%), and 7d (7.33%) also exhibited low cytotoxicity.

2.4. Structure–Activity Relationship of 7a–f

The anti-hepatocellular potential of all of the derivatives, 7a–f, was evaluated against a HepG2 cancer cell line at various concentrations via MTT assay. The most potent derivative was 7f, which contains two methyl groups at ortho-positions of the phenyl ring (IC_{50} value of $16.782 \mu\text{M}$). Compound 7d, which contained an electron-withdrawing Cl-group in an orthogonal position, showed the lowest anti-cancer potency with an IC_{50} value of $39.667 \mu\text{M}$. The anti-proliferative activity of all of the derivatives was decreased in the following order: 7f > 7a > 7b > 7c > 7e > 7d. This proves that the attachment of an electron-donating CH_3 group at the ortho-position increases the anti-cancer activity of the compounds. Based on the results of the SAR of *N*-arylated 5-aryl-1,2,4-triazole-coupled acetamide scaffolds 7a–f, it was determined that the $-\text{CH}_3$ motif at the ortho-position of the phenyl ring improved the anti-proliferative potential of the compounds.

2.5. Molecular Docking

Molecular docking screenings were carried out to theoretically predict the most promising protein targets of compounds by molecular docking to some cancer targets. Five major targets in the treatment of cancer have been identified: human Aurora B kinase, phosphatidylinositol 3-kinase alpha (PI3Kalpha), the signal transducer and activator of transcription 3 (STAT3), protein kinase B (Akt), and c-kit tyrosine kinase (c-Kit). The web page <http://www.swisstargetprediction.ch/> (Accessed on 7 November 2022) was used to study the potential anti-cancer effect of new synthesized molecules [35]. The results suggest that molecules may be effective against kinase targets.

The docking findings demonstrate that all of the compounds have good binding affinity to kinase protein. The protein c-kit tyrosine kinase is expected to interact strongly with cancer-targeted therapeutics. Table 4 shows the docked complexes' categories, modes of interactions, binding affinities, and by-products. Each ligand's hydrophobic contacts and hydrogen bonding interactions were evaluated within the receptor protein's binding pocket.

Table 4. Docking of scaffolds 7a–f to protein c-kit tyrosine kinase.

Ligand	(ACE) (kcal/mol)	Category	Types	Interacting Residues
7a	−173.411	H-bond	Alkyl	LEU595, LYS623, VAL654, LEU644, LEU595, LEU644, CYS673, CYS809, and VAL668.
		Hydrophobic	Pi-alkyl	TYR672.
7b	−167.882	H-bond	Sulfur-X C-alkyl	CYS809. LEU595, VAL654, LEU644, CYS809, LEU595, ILE808, LEU644, AL654.
		Hydrophobic	Pi-alkyl	TYR672, HIS790, and PHE811.
7c	−167.814	H-bond	Conventional	GLU640.
		Hydrophobic	Pi-Alkyl	HIS790. VAL643, VAL603, LYS623, VAL668, LEU783, CYS788, LYS623, LEU644, VAL668, ALA621, and CYS788.
7d	−158.747	H-bond	Conventional	GLU640 and ASP810. ILE808.
		Hydrophobic	C-alkyl Pi-alkyl	VAL603, VAL643, LEU783, CYS788, CYS809, LEU595, VAL603, VAL643, and LEU783.
7e	−161.394	H-bond	Conventional	CYS673, LEU595, VAL654, LEU644,
		Hydrophobic	C-alkyl Pi-alkyl	CYS809, LYS623, LEU644, LEU644, TYR672, and VAL668.
7f	−176.749	H-bond	Conventional H-bond Pi-sigma	GLU640, ASP810, And HIS790.
		Hydrophobic	Alkyl	VAL603, LYS623, VAL643, LEU783, CYS788, LYS623, LEU644, VAL668, CYS809, ILE571, and CYS788.
Reference Ligand		H-bond	Conventional	ALA232, GLU236, MET282, ASP293, GLU279,
STI	−181.533	Other	C-H bond	MET229, GLY159,
		Hydrophobic	C-alkyl	VAL166, LEU158, ALA179, LYS181, and LEU183.

Compound 7f bonded to c-kit tyrosine kinase with the most suitable binding pose and a low binding energy of −176.749 kcal/mol. It formed an H-bond with Asp810 and Glu640. Hydrophobic interactions occurred such as the pi-sigma bond with Thr670, His790, and Val643. Other hydrophobic interactions involved alkyl interactions with Val603, Val668, Leu644, Leu783, and Ile571, pi-sulfur interactions with Cys788 and Lys623, and amide-pi-stacked interactions with Cys809 residue. It also interacts with Val654, Ile789, Leu647, Ile808, Ile653, and Phe811 residues through van der Waals interaction. The 2D and 3D diagrammatic expressions of the binding interactions of 7f and c-kit tyrosine kinase are shown in Figure 5.

According to the docking findings, all triazole-coupled acetamide scaffolds have a significant ability to influence the protein kinase B moiety. Akt is anticipated to have a high affinity for carcinoma therapeutic targets. Table 3 shows the docked complexes' binding interactions, classifications, kinds of interactions, and interacting residues. Each ligand's hydrophobic contacts and hydrogen bonding interactions were assessed within the receptor protein's binding site. Table 5 describes the ligand conformations that demonstrated the greatest biological activity, as well as their suitable interactions in the receptors.

Table 5. Docking of scaffolds 7a–f to protein kinase B.

Ligand	(ACE) (kcal/mol)	Category	Types	Interacting Residues
7a	−166.843	H-bond Other Hydrophobic	Conventional C-H bond Pi-sulfur C-alkyl	GLY164. SER9. PHE163. VAL166, LYS181, and EU183.
7b	−166.371	H-bond Hydrophobic	Conventional C-alkyl	CYS809. LYS181, VAL166, and LEU296.
7c	−162.234	Hydrophobic	Alkyl	LYS181, VAL166, and LEU183.
7d	−154.675	H-bond Hydrophobic	Conventional C-H bond C-alkyl Pi-alkyl	GLY161, LEU158. ASP293. VAL166, LYS181. PHE239, and PHE439.
7e	−156.207	H-bond Hydrophobic	C-H bond Alkyl	CYS673. LEU296.
7f	−170.066	H-bond Hydrophobic	Conventional C-H bond C-alkyl	GLY161, ASP293, and ARG6. ASP293. LYS181 and LEU183.
Reference Ligand		H-bond	Conventional	ALAA232, ASPA293, META282, GLUA279, GLUA236
X39	−130.624	Other Hydrophobic	C-H bond C-alkyl	MET229, GLY159, VAL166, LEU A183, LEU A158, ALA179, LYS and A181.

Compound 7a had the most suitable binding poses with a binding energy of −166.843 kcal/mol to protein kinase B. Compound 7a had the most suitable binding poses with a low energy of −166.843 kcal/mol to the catalytic site of protein kinase B. 7a bonded to protein kinase B via H-bonding with Gly164, Phe163, and Thr162, a carbon–hydrogen bond with SerC9, pi-sigma interaction with Gly161, and pi–sulfur interaction with Asp293. It bonded with residues Leu183, val166, and Lys181 via hydrophobic alkyl interactions. Asn280, Lys277, Glu279, ArgC6, Lys160, Glu236, Gly159, Lys165, and ThrC8 residues involve van der Waals interactions among protein kinase B and compound 7a (Figure 8).

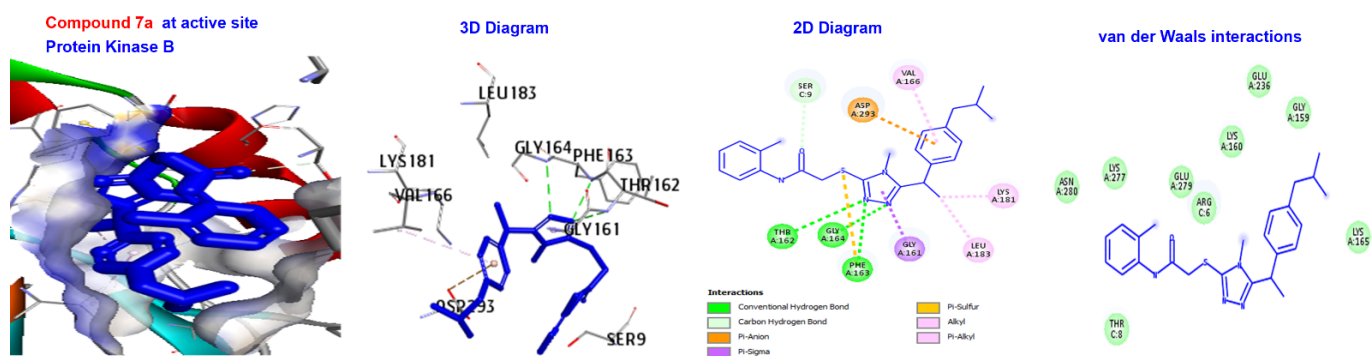


Figure 8. Binding interactions of compound 7a with the protein kinase B binding pocket.

7f and the protein kinase B complex is stabilized by H-bonding and van der Waals interactions. 7f combines with the active site of the protein via H-bonding with Gly161, ArgC6, and Asp293. Hydrophobic bonds are involved with alkyl interactions with Lys181 and Leu183 and pi-sigma interactions with Val166 residues. Figure 9 demonstrates 2D and 3D diagrams displaying the most suitable binding interactions between 7f and the active pocket of the kinase B protein.

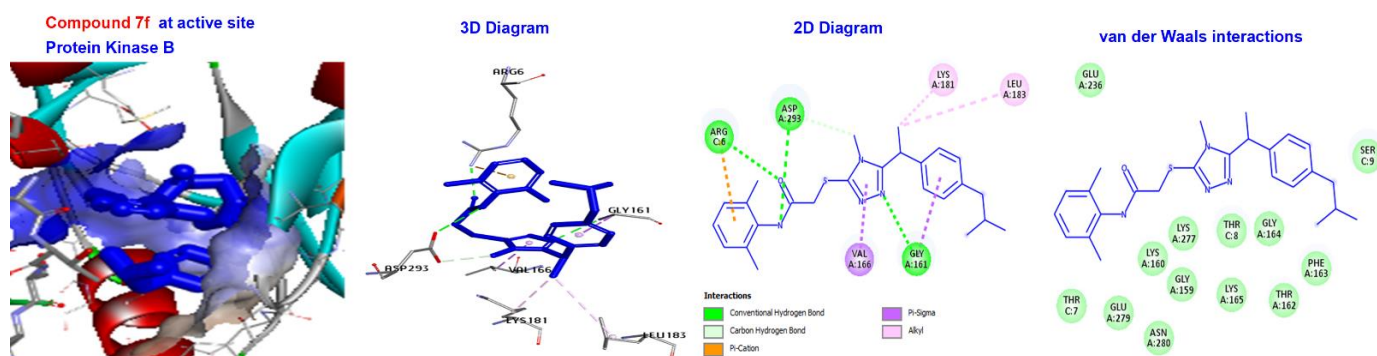


Figure 9. Binding interactions of compound 7f with the protein kinase B binding pocket.

3. Materials and Methods

3.1. General

In the present research, all of the starting materials were of analytical grade and were purchased from Alfa Aesar or Sigma Aldrich. 2-(4-isobutylphenyl) propanoic acid was used as a starting material. A Stuart SMP10 melting point apparatus was used for determining the melting point of all of the derivatives. The structures of all of the triazole-based scaffolds were confirmed by spectroscopy and physicochemical methods. An FT-IR spectrophotometer (4000–400 cm^{-1}) by BRUKER was used at the Hi-Tech Lab, GC University, Faisalabad. ^1H NMR spectra were recorded on an Bruker Advance 500 MHz spectrophotometer using DMSO- d_6 , on 5 mm diameter tubes at the University of Copenhagen, Denmark. An Bruker Advance NMR spectrophotometer was used to record ^{13}C NMR spectra at 75 MHz by using DMSO- d_6 , on 5 mm diameter tubes. The reactions were supervised by thin layer chromatography.

3.2. General Procedure for the Synthesis of Synthesized N-Arylated 5-Aryl-1,2,4-Triazole-Coupled Acetamide Scaffolds 7a–f

3.2.1. Synthesis of Methyl 2-(4-Isobutylphenyl)Propanoate (2)

Compound 2 was prepared by the reported method [42]. The compound (2) was obtained as a pale yellow, oily liquid. Yield: (90%); b.p. 263–265 $^{\circ}\text{C}$; IR (KBr) cm^{-1} : 1736.32, 1203.36, 1162.83; ^1H NMR (400 MHz, CDCl_3) δ 7.15 (d, 2H, J = 8.0 Hz), 7.05 (d, 2H, J = 8.0 Hz), 3.67 (q, 1H), 3.60 (s, 3H), 2.40 (d, 2H, J = 8.0 Hz), 1.82 (m, 1H), 1.44 (d, 3H,

$J = 8.0$ Hz), 0.85 (d, 6H, $J = 8.0$ Hz). ^{13}C NMR (101 MHz, CDCl_3) δ 175.22 (C=O), 140.49 (C-1), 137.63 (C-4), 129.04 (C-2 & C-6), 127.31 (C-3 & C-5), 52.09 (OCH₃), 44.99 (CH₂-9), 40.11 (CH-7), 30.25 (CH-10), 22.21 (CH₃-11 & CH₃-12), 18.50 (CH₃-8). HRMS (ESI+): m/z calculated for $[(\text{C}_{14}\text{H}_{20}\text{O}_2)+\text{H}]^+$: 220.1463; found: 220.1460. Element analysis: C, 76.30; H, 9.16% (Figures S1 and S6).

3.2.2. Synthesis of 2-(4-Isobutylphenyl)Propanehydrazide (3)

Compound **3** was prepared by the reported method [43]. 2-(4-isobutylphenyl) propane hydrazide was separated as a white, crystalline solid. Yield: (88%); m.p. 77–78 °C; IR (KBr) cm^{-1} : 3272.76, 2963.13, 1640.12, 1604.83, 1466.29, 1366.62, 906.66, 686.83. ^1H NMR (400 MHz, CDCl_3) δ 9.50 (s, 1H), 7.13 (d, 2H, $J = 8.0$ Hz), 7.06 (d, 2H, $J = 8.0$ Hz), 3.48 (d, 2H), 3.46 (q, 1H), 2.40 (d, 2H, $J = 8.0$ Hz), 1.81 (m, 1H), 1.48 (d, 3H, $J = 8.0$ Hz), 0.84 (d, 6H, $J = 8.0$ Hz). ^{13}C NMR (101 MHz, CDCl_3) δ 175.24 (C=O), 140.49 (C-1), 137.59 (C-4), 129.57 (C-2 & C-6), 127.30 (C-3 & C-5), 44.96 (CH₂-9), 40.11 (CH-7), 30.25 (CH-10), 22.19 (CH₃-11 & CH₃-12), 18.23 (CH₃-8). HRMS (ESI+): m/z calculated for $[(\text{C}_{13}\text{H}_{20}\text{N}_2\text{O})+\text{H}]^+$. 220.1576; found: 220.1574. Element analysis: C, 70.85; H, 9.16; N, 12.72% (Figures S2 and S7).

3.2.3. Synthesis of 5-(1-(4-Isobutylphenyl)Ethyl)-1,2,4-Triazole-2-Thiol (4)

In the current study, methyl isothiocyanate and 2-(4-isobutylphenyl) propane hydrazide (0.02 mol) were dissolved in 10% KOH soln. in an equimolar amount. For 10–11 h, the mixture was set on refluxing at 95 °C. Thin-layer chromatography was used for monitoring the reaction. Upon completion, cold water was added to afford the precipitates of product. Water was used to filter and wash the precipitates. The precipitates were further purified with an ethanolic recrystallization process. The 5-(1-(4-isobutylphenyl)ethyl)-1,2,4-triazole-2-thiol scaffold was crystallized as an off-white solid. ^1H NMR (400 MHz, CDCl_3) δ 11.77 (s, 1H, SH), 7.05 (d, 2H, $J = 8.0$ Hz), 6.99 (d, 2H, $J = 8.0$ Hz), 3.96 (q, 1H), 3.18 (s, 3H), 2.39 (d, 2H, $J = 8.0$ Hz), 1.80 (m, 1H), 1.62 (d, 3H, $J = 8.0$ Hz), 0.83 (d, 6H, $J = 8.0$ Hz). ^{13}C NMR (101 MHz, CDCl_3) 155.16 (C-1 & C-4), 141.43 (C-1), 137.11 (C-4), 129.94 (C-2 & C-6), 126.87 (C-3 & C-5), 45.03 (CH₂-9), 37.60 (CH-7), 30.67 (CH-10), 30.15 (CH₃-N), 22.22 (CH₃-11 & CH₃-12), 20.20 (CH₃-8). HRMS (ESI+): m/z calculated for $[(\text{C}_{15}\text{H}_{21}\text{N}_3\text{S})+\text{H}]^+$: 275.1456; found: 275.1454. Element analysis: C, 65.41; H, 7.69; N, 15.27; S, 11.65% (Figures S3–S5 and S8).

3.2.4. Synthesis of N-Aryl/Alkyl 2-Bromoacetamides 6a–f

Compounds **6a–f** were synthesized using the reported method [27]. In an RBF, 12.0 moles N-substituted alkyl/aryl amines (**5a–f**) were dissolved in 10.0 mL of 5% Na_2CO_3 solution. Bromoacetyl bromide (12.0 mmoles) was gradually added to the reaction mixture described above. Upon reaction completion, n-hexane was added to afford arylated derivatives as precipitates which were further purified with an ethanolic recrystallization process or column chromatography technique using ethyl acetate–petroleum ether (1:9).

3.2.5. Synthesis of N-Arylated 5-(1-(4-Isobutylphenyl)Ethyl)-1,2,4-Triazole-2-yl-2-Sulfanyl Coupled Acetamide Derivatives 7a–f

Various N-arylated 5-(1-(4-isobutylphenyl)ethyl)-1,2,4-triazole-2-yl-2-sulfanyl-coupled acetamide compounds were prepared in good yield by thoroughly mixing **4** (0.02 mol) with an equimolar amount of N-alkyl/aryl 2-bromoacetamides **6a–f** using DMF and NaH (0.01 mol). Thin-layer chromatography was used for monitoring the reaction. Upon reaction completion, n-hexane was added to afford arylated derivatives as precipitates which were further purified with an ethanolic recrystallization process or column chromatography technique using ethyl acetate–petroleum ether (1:9).

3.2.6. *N*-(2-Methylphenyl)-2-((5-(1-(4-isobutylphenyl)ethyl)-4-methyl-4H-1,2,4-triazol-3-yl)thio)Acetamide (**7a**)

White, amorphous solid. Yield 73%, m.p 122–124 °C. IR: ν (cm⁻¹): 3270, 1696, 1524, 1488, 1306, 1082, 756. ¹HNMR (500 MHz, DMSO) δ 9.64 (s, 1H), 7.40 (d, *J* = 5.0 Hz), 7.20 (d, *J* = 5.0 Hz), 7.15 (t, 1H), 7.09–7.06 (m, 5H), 4.33–4.29 (q, 1H), 4.04 (s, 2H), 3.28 (s, 3H), 2.40 (d, 2H, *J* = 10.0 Hz), 2.15 (s, 3H), 1.83–1.78 (m, 1H) 1.60 (d, *J* = 5.0 Hz), 0.85 (d, *J* = 10.0 Hz). ¹³C NMR (126 MHz, DMSO) δ 165.93, 158.08, 149.15, 139.59, 139.36, 135.90, 131.21, 130.27, 129.27, 126.81, 125.92, 125.18, 124.32, 44.15, 37.11, 35.47, 29.99, 29.53, 22.14, 20.93, 17.67 (Figures S9–S11). HRMS (ESI+): *m/z* calculated for [(C₂₄H₃₀N₄OS)+H]⁺: 423.2119; found: 423.2214 (Figure S27). Analysis calculated for C₂₄H₃₀N₄OS, C, 68.21; H, 7.16; N, 13.26; S, 7.59%.

3.2.7. *N*-(4-Bromo-2-Methylphenyl)-2-((5-(1-(4-Isobutylphenyl)Ethyl)-4-Methyl-4H-1,2,4-Triazol-3-yl)Thio)Acetamide (**7b**)

Off-white, amorphous solid. m.p 122–124 °C. Yield 71%. IR: ν (cm⁻¹): 3370, 1670, 1528, 1470, 1306, 659.93. ¹HNMR (500 MHz, DMSO) δ 9.68 (s, 1H), 7.43 (s, 1H), 7.40 (d, *J* = 5.0 Hz, 1H), 7.34 (dd, *J* = 10.0 Hz, 1H), 7.08–7.05 (m, 4H), 4.33–4.2 (q, 1H), 4.04 (s, 2H), 3.27 (s, 3H), 2.40 (d, 2H, *J* = 10.0 Hz), 2.15 (s, 3H), 1.80–1.75 (m, 1H), 1.60 (d, *J* = 10.0 Hz, 3H), 0.85 (d, *J* = 10.0 Hz, 6H). ¹³C NMR (126 MHz, DMSO) δ 166.17, 158.09, 149.05, 139.53, 139.30, 135.34, 133.77, 132.67, 129.25, 128.71, 126.78, 125.93, 44.15, 37.10, 35.47, 30.00, 29.53, 22.14, 20.92, 17.40 (Figures S12–S14). HRMS (ESI+): *m/z* calculated for [(C₂₄H₂₉BrN₄OS)+H]⁺: 501.1324; found: 503.1313 (Figure S28). Analysis calculated for C₂₄H₂₉BrN₄OS. Elemental Analysis: C, 57.48; H, 5.83; N, 11.17; S, 6.39.

3.2.8. *N*-(4-Ethylphenyl)-2-((5-(1-(4-Isobutylphenyl)Ethyl)-4-Methyl-4H-1,2,4-Triazol-3-yl)Thio)Acetamide (**7c**)

Off-white, amorphous solid. Yield 75%, m.p 100–102 °C. IR: ν (cm⁻¹): 3235, 1682, 1517, 1468, 1320, 695. ¹HNMR (500 MHz, DMSO) δ 10.18 (s, 1H), 7.43–7.42 (d, 2H, *J* = 5.0 Hz), 7.14–7.13 (d, 2H, *J* = 5.0 Hz), 7.05–7.01, (m, 4H), 4.32–4.29 (q, 1H), 3.98 (s, 2H), 3.26 (s, 3H), 2.39(d, 2H, *J* = 5.0 Hz), 1.81–1.76 (m, 1H), 1.59 (d, *J* = 12, 3H), 1.17–1.14 (t, 3H) 0.84 (d, *J* = 5.0 Hz, 6H). ¹³C NMR (126 MHz, DMSO) δ 165.44, 157.97, 149.05, 139.46, 139.35, 138.87, 136.40, 129.25, 127.91, 126.68, 119.14, 44.15, 37.84, 35.49, 29.97, 29.52, 27.54, 22.14, 20.89, 15.60 (Figures S15–S17). HRMS (ESI+): *m/z* calculated for [(C₂₅H₃₂N₄OS)+H]⁺: 437.2375; found: 437.2366 (Figure S29). Analysis calculated for C₂₅H₃₂N₄OS, C, 68.77; H, 7.39; N, 12.83; S, 7.34.

3.2.9. *N*-(2-Chlorophenyl)-2-((5-(1-(4-Isobutylphenyl)Ethyl)-4-Methyl-4H-1,2,4-Triazol-3-yl)Thio)Acetamide (**7d**)

White, amorphous solid. Yield 70%, m.p 123–125 °C. IR: ν (cm⁻¹): 3330, 1691, 1515, 1452, 1315, 1081, 757. ¹HNMR (500 MHz, DMSO) δ 9.90 (s, 1H), 7.75 (d, 1H, *J* = 10.0 Hz), 7.50 (d, 1H, *J* = 10.0 Hz), 7.33–7.31 (t, 1H, *J* = 5.0 & 10.0 Hz), 7.21–7.18 (t, 1H, *J* = 5.0 & 10.0 Hz), 7.10–7.06 (m, 4H), 4.33–4.29 (q, 1H), 4.12 (s, 2H), 3.28 (s, 3H), 2.40(d, 2H, *J* = 5.0 Hz), 1.79–1.76 (m, 1H) 1.60 (d, *J* = 5.0 Hz, 3H), 0.84 (d, *J* = 10.0 Hz, 6H). ¹³C NMR (126 MHz, DMSO) δ 166.56, 158.12, 148.93, 139.65, 139.28, 134.53, 129.50, 129.27, 127.43, 126.81, 126.14, 125.14, 44.07, 37.07, 35.48, 30.04, 29.53, 22.13, 20.97 (Figures S18–S20). HRMS (ESI+): *m/z* calculated for [(C₂₃H₂₇ClN₄OS)+H]⁺: 444.1672; found: 444.1697 (Figure S30). Analysis calculated for C₂₃H₂₇ClN₄OS, C, 62.36; H, 6.14; N, 12.65; S, 7.24.

3.2.10. *N*-(Phenyl)-2-((5-(1-(4-Isobutylphenyl)Ethyl)-4-Methyl-4H-1,2,4-Triazol-3-yl)Thio)Acetamide (**7e**)

White, amorphous solid. Yield 74%, m.p 88–90 °C. IR: ν (cm⁻¹): 3250, 1686, 1525, 1436, 1303, 1082, 757. ¹HNMR (500 MHz, DMSO) δ 10.27 (s, 1H), 7.54 (d, 2H, *J* = 10.0 Hz), 7.32–7.29 (t, 2H, *J* = 5.0 & 10.0 Hz), 7.10–7.02 (m, 5H), 4.31–4.29 (q, 1H), 4.01 (s, 2H), 3.29 (s, 3H), 2.39(d, 2H, *J* = 5.0 Hz), 1.79–1.76 (m, 1H), 1.59 (d, *J* = 5.0 Hz, 3H), 0.85 (d, *J* = 10.0 Hz, 6H).

^{13}C NMR (126 MHz, DMSO), δ 165.75, 158.10, 149.03, 139.60, 139.33, 138.68, 129.25, 128.74, 126.77, 123.42, 119.04, 44.10, 37.79, 35.41, 29.88, 29.49, 22.14, 20.89 (Figures S21–S23). HRMS (ESI+): m/z calculated for $[(\text{C}_{23}\text{H}_{28}\text{N}_4\text{OS})+\text{H}]^+$: 409.2044; found: 409.2054 (Figure S31). Analysis calculated for $\text{C}_{23}\text{H}_{28}\text{N}_4\text{OS}$, C, 67.62; H, 6.91; N, 13.71; S, 7.85.

3.2.11. *N*-(2,6-Dimethylphenyl)-2-((5-(1-(4-Isobutylphenyl)Ethyl)-4-Methyl-4H-1,2,4-Triazol-3-yl)Thio)Acetamide (7f)

Off-white, amorphous solid. Yield 76%, m.p 150–152 °C. IR: ν (cm^{-1}): 3272, 1640, 1516, 1445, 1388, 1081, 694. ^1H NMR (500 MHz, DMSO) δ 9.68 (s, 1H), 7.12–7.02 (m, 7H), 4.40–4.23 (q, 1H), 4.06 (s, 2H), 3.29 (s, 3H), 2.29 (d, 2H, $J = 10.0$ Hz), 2.13 (s, 6H), 1.81–1.78 (m, 1H), 1.61 (d, $J = 5.0$ Hz, 3H), 0.85 (d, $J = 10.0$ Hz, 6H). ^{13}C NMR (126 MHz, DMSO) δ 165.46, 157.98, 149.10, 139.60, 139.38, 135.06, 134.57, 129.26, 127.57, 126.83, 126.49, 44.15, 36.59, 35.46, 29.97, 29.54 (Figures S24–S26). HRMS (ESI+): m/z calculated for $[(\text{C}_{25}\text{H}_{32}\text{N}_4\text{OS})+\text{H}]^+$: 437.2375; found: 437.2366 (Figure S32). Analysis calculated for $\text{C}_{25}\text{H}_{32}\text{N}_4\text{OS}$, C, 68.77; H, 7.39; N, 12.83; S, 7.34.

3.3. Experimental Procedures for Biological Activities

3.3.1. Cell Culture and Treatment

Human HepG2 liver cancer cell lines were cultured by Dulbecco's modified Eagle's medium. It is composed of 100 $\mu\text{g}/\text{mL}$ streptomycin, 100 units/mL penicillin, and 10% FBS. A humidified atmosphere was provided for incubation at 37 °C with 5% CO_2 . The anti-hepatocellular therapeutic potential of triazole-based scaffolds was evaluated by dissolving its different concentrations in 0.05% DMSO.

3.3.2. Evaluation of Cell Viability

An MTT assay was applied for evaluation of cell viability against the HepG2 cell line [44]. In short, different concentrations of new triazole-based scaffolds were incubated with HepG2 cell lines for 48 h. After incubation, 5 mg/mL of 10 μL MTT solution was added in each plate and they were further incubated at 37 °C for 4 h. The percentage of cell viability was calculated at 490 nm after the addition of 150 μL DMSO into a microplate reader (Thermo Scientific, Waltham, MA, USA).

3.3.3. Hemolytic Activity Potential

Hemolytic activity was investigated by the reported method [45,46] using Triton-X-100 as standard.

3.4. Molecular Docking of Triazole-Coupled Acetamides

Docking experiments for all of the scaffolds were carried out in order to comprehend the potential interaction process of the synthesized anti-cancer compounds on the HepG2 cancer cell line. The website <https://www.rcsb.org> was used for drawing the structures of PI3K α , Akt, c-kit tyrosine kinase, human Aurora B kinase, and STAT3 from the RCSB Protein Data Bank under the PDB IDs of 4FA6, 2X39, 1T46, 4AF3, and 6NJS, respectively [36–39,47]. ChemDraw 20.1.1 was used to create and reduce the 3D SDF structures of all of the compounds, which were then transferred to MarvinSketch. Prior to docking, the target proteins' frameworks were evaluated, and errors in amino acid structures were rectified using Molegro Virtual Docker software [48]. The grid boxes' centers were chosen to be the co-crystallized ligands of proteins. They re-docked in order to validate the in silico process. Molegro Virtual Docker was applied to dock active chemicals 10 times to the target proteins' receptors. The sequences with the lowest interaction affinity and excellent connections with the targets were separated for further detailed analysis. The molecular bindings between the target and new derivatives were visualized in 2D using Discovery Studio Visualizer Software 2021.

4. Conclusions

A series of new anti-cancer compounds (**7a–f**) were synthesized in moderate to good yield (73–76%) by combining compound **4** with various electrophiles under different reaction conditions (Table 1, Scheme 1). Because of its low bioavailability of 38–49%, Sorafenib necessitates a significant daily dose in cancer therapy. Sorafenib is a very costly medicine with many side effects. We have incorporated various electron-donating and electron-withdrawing groups into electrophiles to test structure–activity relationships at various concentrations. All of the molecules demonstrated medium to outstanding anti-cancer activity, comparable to sorafenib, which diversified according to aryl ring substitution, as shown in Table 1. These triazole-based acetamide derivatives also exhibited low cytotoxicity, with values ranging from 7.33% to 1.19% in comparison to the 100% cytotoxicity exhibited by the reference standard Triton X100. Compounds **7f** and **7a** showed the highest anti-cancer potential, with IC₅₀ values of 16.782 µg/mL and 20.667 µg/mL, respectively. On the other hand, the triazole derivative containing an electron-withdrawing chloro moiety demonstrated the least anti-proliferative activity with an IC₅₀ value of 39.667 µg/mL. The sequence of anti-cancer potential was found to be **7f** > **7a** > **7b** > **7c** > **7e** > **7d**. The anti-cancer potential of all of the compounds was further investigated by molecular docking studies and the results were in accordance with in-vitro studies. In silico studies have shown that the molecules have strong affinity for kinase targets. Molecules **7f** and **7a** have shown their anti-cancer effects, especially by affecting Akt and c-lit molecular targets. According to in silico modelling studies, **7f** has an outstanding docking score with the lowest binding energy of −170.066 kcal/mol, which is lower than the reference ligand X39 for protein kinase B (−130.624 kcal/mol). We concluded that compound **7f** contained electron-donating methyl groups at the 2 and 6 position of the aryl ring and showed good anti-cancer activity, low cytotoxicity, and good thrombolytic activity. Thus, compound **7f** might be utilized to synthesize new anti-cancer drugs in the near future.

Supplementary Materials: The following supporting information can be downloaded at: <https://www.mdpi.com/article/10.3390/ph16020211/s1>, Figure S1: 1HNMR spectrum of compound 2, Figure S2: 1HNMR spectrum of compound 3, Figure S3: 1HNMR spectrum of compound 4, Figure S4: 1HNMR spectrum of compound 4 (aromatic region), Figure S5: 1HNMR spectrum of compound 4 (aliphatic region), Figure S6: 13C NMR spectrum of compound 2, Figure S7: 13C NMR spectrum of compound 3, Figure S8: 13C NMR spectrum of compound 4, Figure S9: 1H NMR spectrum of 7a, Figure S10: COSYH NMR spectrum of 7a, Figure S11: 13C NMR spectrum of 7a, Figure S12: 1H NMR spectrum of 7b, Figure S13: COSYH NMR spectrum of 7b, Figure S14: 13C NMR spectrum of 7b, Figure S15: 1H NMR spectrum of 7c, Figure S16: COSYH NMR spectrum of 7c, Figure S17: 13C NMR spectrum of 7c, Figure S18: 1H NMR spectrum of 7d, Figure S19: COSYH NMR spectrum of 7d, Figure S20: 13C NMR spectrum of 7d, Figure S21: 1H NMR spectrum of 7e, Figure S22: COSYH NMR spectrum of 7e, Figure S23: 13C NMR spectrum of 7e, Figure S24: 1H NMR spectrum of 7f, and Figure S25: COSYH NMR spectrum of 7f. Figure S26: 13C NMR spectrum of 7f. Figure S27: HRMS spectrum of compound 7a, Figure S28: HRMS spectrum of compound 7b, Figure S29: HRMS spectrum of compound 7c, Figure S30: HRMS spectrum of compound 7d, Figure S31: HRMS spectrum of compound 7e, and Figure S32: HRMS spectrum of compound 7f.

Author Contributions: Conceptualization and experimental design, S.G.K. and S.A.A.S.; methodology, N.A., S.I., S.G.K. and M.A.S.A.; experimental work, S.B., S.G.K., Ş.A., A.u.R., F.A. and S.M.; software, J.B.C. and Ş.A.; writing—original draft preparation, N.A., S.B., A.R., Z.R., S.G.K. and M.A.S.A.; writing—review and editing, Ş.A., Z.R., N.A., A.u.R., S.B., S.G.K., M.u.N., Z.R., J.B.C., A.R., S.A.A.S., F.A. and M.A.S.A.; data curation, J.B.C., S.I., S.M., S.A.A.S., F.A., N.R., Z.R., M.u.N. and S.G.K.; visualization, S.G.K., A.u.R., Ş.A., M.u.N. and J.B.C.; supervision, S.G.K.; project administration, S.G.K., N.A. and M.A.S.A.; funding acquisition, S.A.A.S. All authors have read and agreed to the published version of the manuscript.

Funding: The authors would like to acknowledge the Ministry of Higher Education (MOHE) Malaysia for financial support under the Fundamental Research Grant Scheme (FRGS) with sponsorship reference number FRGS/1/2019/STG05/UITM/02/9. The authors would also like to acknowledge the Universiti Teknologi MARA for the financial support under the reference number 600-IRMI/FRGS 5/3 (424/2019).

Institutional Review Board Statement: Not applicable.

Informed Consent Statement: Not applicable.

Data Availability Statement: Data is contained within the article and Supplementary Material.

Acknowledgments: The authors would like to acknowledge Research Management Centre (RMC), Office of Deputy Vice-Chancellor (Research & Innovation), Universiti Teknologi MARA 40450 Shah Alam Selangor Darul Ehsan Malaysia for financial support.

Conflicts of Interest: The authors declare no conflict of interest.

Sample Availability: Samples of all of the compounds are available from the authors.

References

1. Kamal, A.; Bharathi, E.V.; Reddy, J.S.; Ramaiah, M.J.; Dastagiri, D.; Reddy, M.K.; Viswanath, A.; Reddy, T.L.; Shaik, T.B.; Pushpavalli, S.; et al. Synthesis and biological evaluation of 3,5-diaryl isoxazoline/isoxazole linked 2,3-dihydroquinazolinone hybrids as anticancer agents. *Eur. J. Med. Chem.* **2011**, *46*, 691–703. [[CrossRef](#)] [[PubMed](#)]
2. Tahiliani, H.T.; Purohit, A.P.; Desai, S.C.; Jarwani, P.B. Retrospective analysis of histopathological spectrum of premalignant and malignant colorectal lesions. *Cancer Res. Stat. Treat.* **2021**, *4*, 472–478. [[CrossRef](#)]
3. Jang, J.-W.; Song, Y.; Kim, K.M.; Kim, J.-S.; Choi, E.K.; Kim, J.; Seo, H. Hepatocellular carcinoma-targeted drug discovery through image-based phenotypic screening in co-cultures of HCC cells with hepatocytes. *BMC Cancer* **2016**, *16*, 810. [[CrossRef](#)] [[PubMed](#)]
4. Rungay, H.; Arnold, M.; Ferlay, J.; Lesi, O.; Cabasag, C.J.; Vignat, J.; Laversanne, M.; McGlynn, K.A.; Soerjomataram, I. Global burden of primary liver cancer in 2020 and predictions to 2040. *J. Hepatol.* **2022**, *77*, 1598–1606. [[CrossRef](#)]
5. Zheng, Z.; Liu, Q.; Kim, W.; Tharmalingam, N.; Fuchs, B.B.; Mylonakis, E. Antimicrobial activity of 1,3,4-oxadiazole derivatives against planktonic cells and biofilm of *Staphylococcus aureus*. *Futur. Med. Chem.* **2018**, *10*, 283–296. [[CrossRef](#)] [[PubMed](#)]
6. Hanahan, D.; Weinberg, R.A. Hallmarks of cancer: The next generation. *Cell* **2011**, *144*, 646–674. [[CrossRef](#)]
7. Chen, J.-S.; Chou, C.-H.; Wu, Y.-H.; Yang, M.-H.; Chu, S.-H.; Chao, Y.-S.; Chen, C.-N. CC-01 (chidamide plus celecoxib) modifies the tumor immune microenvironment and reduces tumor progression combined with immune checkpoint inhibitor. *Sci. Rep.* **2022**, *12*, 1100. [[CrossRef](#)]
8. Liu, Q.; Zhang, B.; Wang, Y.; Wang, X.; Gou, S. Discovery of phthalazino[1,2-b]-quinazolinone derivatives as multi-target HDAC inhibitors for the treatment of hepatocellular carcinoma via activating the p53 signal pathway. *Eur. J. Med. Chem.* **2021**, *229*, 114058. [[CrossRef](#)]
9. Chen, C.; Li, X.; Zhao, H.; Liu, M.; Du, J.; Zhang, J.; Yang, X.; Hou, X.; Fang, H. Discovery of DNA-Targeting HDAC Inhibitors with Potent Antitumor Efficacy In Vivo That Trigger Antitumor Immunity. *J. Med. Chem.* **2022**, *65*, 3667–3683. [[CrossRef](#)]
10. Khan, I.; Ibrar, A.; Abbas, N.; Saeed, A. Recent advances in the structural library of functionalized quinazoline and quinazolinone scaffolds: Synthetic approaches and multifarious applications. *Eur. J. Med. Chem.* **2014**, *76*, 193–244. [[CrossRef](#)]
11. Khwaza, V.; Mlala, S.; Oyedeji, O.; Aderibigbe, B. Pentacyclic Triterpenoids with Nitrogen-Containing Heterocyclic Moiety, Privileged Hybrids in Anticancer Drug Discovery. *Molecules* **2021**, *26*, 2401. [[CrossRef](#)] [[PubMed](#)]
12. Gomha, S.M.; Abdel-Aziz, H.M.; El-Reedy, A.A.M. Facile Synthesis of Pyrazolo[3,4-c]pyrazoles Bearing Coumarine Ring as Anticancer Agents. *J. Heterocycl. Chem.* **2018**, *55*, 1960–1965. [[CrossRef](#)]
13. Kaproń, B.; Czarnomysy, R.; Wysokiński, M.; Andrys, R.; Musilek, K.; Angeli, A.; Supuran, C.T.; Plech, T. 1,2,4-Triazole-based anticonvulsant agents with additional ROS scavenging activity are effective in a model of pharmacoresistant epilepsy. *J. Enzym. Inhib. Med. Chem.* **2020**, *35*, 993–1002. [[CrossRef](#)] [[PubMed](#)]
14. Li, Y.-S.; Tian, H.; Zhao, D.-S.; Hu, D.-K.; Liu, X.-Y.; Jin, H.-W.; Song, G.-P.; Cui, Z.-N. Synthesis and bioactivity of pyrazole and triazole derivatives as potential PDE4 inhibitors. *Bioorganic Med. Chem. Lett.* **2016**, *26*, 3632–3635. [[CrossRef](#)]
15. de Andrade, M.A.R.; Lima, B.J.S.; de Jesus, A.A.; Teixeira, L.D.A.C.; de Souza, C.R.S.; Fontes, R.B.; Mendonça, N.P.V.; Gonçalves, H.S.; Cesar, A.S.; Aragão, M.T. Burnout Syndrome in COVID-19: An analysis of physicians from the public and private health system in the state of Sergipe. *Res. Soc. Dev.* **2022**, *11*, e3911729602. [[CrossRef](#)]
16. Kumar, S.; Khokra, S.L.; Yadav, A. Triazole analogues as potential pharmacological agents: A brief review. *Futur. J. Pharm. Sci.* **2021**, *7*, 106. [[CrossRef](#)]
17. Han, S.; Zhang, F.-F.; Xie, X.; Chen, J.-Z. Design, synthesis, biological evaluation, and comparative docking study of 1,2,4-triazolones as CB1 receptor selective antagonists. *Eur. J. Med. Chem.* **2014**, *74*, 73–84. [[CrossRef](#)]
18. Zhang, W.; Yuan, J. Poly(1-Vinyl-1,2,4-triazolium) Poly(Ionic Liquid)s: Synthesis and the Unique Behavior in Loading Metal Ions. *Macromol. Rapid Commun.* **2016**, *37*, 1124–1129. [[CrossRef](#)]

19. Cao, X.; Wang, W.; Wang, S.; Bao, L. Asymmetric synthesis of novel triazole derivatives and their in vitro antiviral activity and mechanism of action. *Eur. J. Med. Chem.* **2017**, *139*, 718–725. [[CrossRef](#)]
20. Hu, G.; Wang, C.; Xin, X.; Li, S.; Li, Z.; Zhao, Y.; Gong, P. Design, synthesis and biological evaluation of novel 2,4-diaminopyrimidine derivatives as potent antitumor agents. *New J. Chem.* **2019**, *43*, 10190–10202. [[CrossRef](#)]
21. Ni, T.; Ding, Z.; Xie, F.; Hao, Y.; Bao, J.; Zhang, J.; Yu, S.; Jiang, Y.; Zhang, D. Design, Synthesis, and In Vitro and In Vivo Antifungal Activity of Novel Triazoles Containing Phenylethynyl Pyrazole Side Chains. *Molecules* **2022**, *27*, 3370. [[CrossRef](#)] [[PubMed](#)]
22. Zhang, G.-F.; Liu, X.; Zhang, S.; Pan, B.; Liu, M.-L. Ciprofloxacin derivatives and their antibacterial activities. *Eur. J. Med. Chem.* **2018**, *146*, 599–612. [[CrossRef](#)] [[PubMed](#)]
23. Li, Z.; Xu, L.; Zhu, L.; Zhao, Y.; Hu, T.; Yin, B.; Liu, Y.; Hou, Y. Design, synthesis and biological evaluation of novel pteridinone derivatives possessing a hydrazone moiety as potent PLK1 inhibitors. *Bioorganic Med. Chem. Lett.* **2020**, *30*, 127329. [[CrossRef](#)] [[PubMed](#)]
24. Akhtar, T.; Hameed, S.; Al-Masoudi, N.P.; Khan, K.M. Synthesis and anti-HIV activity of new chiral 1,2,4-triazoles and 1,3,4-thiadiazoles. *Heteroat. Chem.* **2007**, *18*, 316–322. [[CrossRef](#)]
25. Irfan, A.; Faiz, S.; Rasul, A.; Zafar, R.; Zahoor, A.F.; Kotwica-Mojzycz, K.; Mojzycz, M. Exploring the Synergistic Anticancer Potential of Benzofuran–Oxadiazoles and Triazoles: Improved Ultrasound- and Microwave-Assisted Synthesis, Molecular Docking, Hemolytic, Thrombolytic and Anticancer Evaluation of Furan-Based Molecules. *Molecules* **2022**, *27*, 1023. [[CrossRef](#)]
26. Gul, S.; Rehman, A.U.; Abbasi, M.A.; Khan, K.M.; Nafeesa, K.; Siddiq, A.; Akhtar, M.N.; Shahid, M.; Subhani, Z. Synthesis, antimicrobial evaluation and hemolytic activity of 2-[[5-alkyl/aralkyl substituted-1,3,4-oxadiazol-2-yl]thio]-N-[4-(4-morpholinyl)phenyl]acetamide derivatives. *J. Saudi Chem. Soc.* **2014**, *21*, S425–S433. [[CrossRef](#)]
27. Khan, S.G.; Bokhari, T.H.; Anjum, F.; Akhter, N.; Rasool, S.; Shah, S.A.A.; Shahid, M.; Arshad, A. Synthesis, characterization, antibacterial, hemolytic and thrombolytic activity evaluation of 5-(3-chlorophenyl)-2-((N-(substituted)-2-acetamoyl) sulfanyl)-1, 3, 4-oxadiazole derivatives. *Pak. J. Pharm. Sci.* **2020**, *33*, 871–876.
28. Mahmood, S.; Khan, S.G.; Rasul, A.; Christensen, J.B.; Abourehab, M.A.S. Ultrasound Assisted Synthesis and In Silico Modelling of 1,2,4-Triazole Coupled Acetamide Derivatives of 2-(4-Isobutyl phenyl)propanoic acid as Potential Anticancer Agents. *Molecules* **2022**, *27*, 7984. [[CrossRef](#)]
29. Aziz-ur-Rehman; Khan, S.G.; Naqvi, S.A.R.; Ahmad, M.; Akhtar, N.; Bokhari, T.H.; Irfan, M.; Usman, A.; Batool, S.; Rasool, S. Synthesis, spectral analysis and biological evaluation of 2-[(morpholin-4-yl) ethyl] thio]-5-phenyl/aryl-1, 3, 4-oxadiazole derivatives. *Pak. J. Pharm. Sci.* **2021**, *34*, 441–446. [[CrossRef](#)]
30. Amewu, R.K.; Sakyi, P.O.; Osei-Safo, D.; Addae-Mensah, I. Synthetic and Naturally Occurring Heterocyclic Anticancer Compounds with Multiple Biological Targets. *Molecules* **2021**, *26*, 7134. [[CrossRef](#)]
31. Zabiulla; Gulnaz, A.; Mohammed, Y.H.E.; Khanum, S.A. Design, synthesis and molecular docking of benzophenone conjugated with oxadiazole sulphur bridge pyrazole pharmacophores as anti-inflammatory and analgesic agents. *Bioorganic Chem.* **2019**, *92*, 103220. [[CrossRef](#)] [[PubMed](#)]
32. Iqbal, K.; Jamal, Q.; Iqbal, J.; Afreen, M.S.; Sandhu, M.Z.A.; Dar, E.; Farooq, U.; Mushtaq, M.F.; Arshad, N.; Iqbal, M.M. Synthesis of N-substituted acetamide derivatives of azinane-bearing 1,3,4-oxadiazole nucleus and screening for antibacterial activity. *Trop. J. Pharm. Res.* **2017**, *16*, 429. [[CrossRef](#)]
33. Thongnest, S.; Chawengrum, P.; Keeratchamroen, S.; Lirdpramongkol, K.; Eurtivong, C.; Boonsombat, J.; Kittakooop, P.; Svasti, J.; Ruchirawat, S. Vernodalidimer L, a sesquiterpene lactone dimer from *Vernonia extensa* and anti-tumor effects of vernodalin, vernolepin, and vernolide on HepG2 liver cancer cells. *Bioorganic Chem.* **2019**, *92*, 103197. [[CrossRef](#)] [[PubMed](#)]
34. Shahzadi, I.; Parveen, B.; Ahmad, S.; Zahoor, A.F.; Rasul, A.; Zahid, F.M. In-vitro cytotoxic evaluation, hemolytic and thrombolytic potential of newly designed acefylline based hydrazones as potent anti-cancer agents against human lung cancer cell line (A549). *Pak. J. Pharm. Sci.* **2022**, *35*, 885–889. [[PubMed](#)]
35. Daina, A.; Michielin, O.; Zoete, V. SwissTargetPrediction: Updated data and new features for efficient prediction of protein targets of small molecules. *Nucleic Acids Res.* **2019**, *47*, W357–W364. [[CrossRef](#)] [[PubMed](#)]
36. Mol, C.D.; Dougan, D.R.; Schneider, T.R.; Skene, R.J.; Kraus, M.L.; Scheibe, D.N.; Snell, G.P.; Zou, H.; Sang, B.-C.; Wilson, K.P. Structural Basis for the Autoinhibition and STI-571 Inhibition of c-Kit Tyrosine Kinase. *J. Biol. Chem.* **2004**, *279*, 31655–31663. [[CrossRef](#)] [[PubMed](#)]
37. McHardy, T.; Caldwell, J.J.; Cheung, K.-M.; Hunter, L.J.; Taylor, K.; Rowlands, M.; Ruddle, R.; Henley, A.; Brandon, A.D.H.; Valenti, M.; et al. Discovery of 4-Amino-1-(7H-pyrrolo[2,3-d]pyrimidin-4-yl)piperidine-4-carboxamides As Selective, Orally Active Inhibitors of Protein Kinase B (Akt). *J. Med. Chem.* **2010**, *53*, 2239–2249. [[CrossRef](#)] [[PubMed](#)]
38. Elkins, J.M.; Santaguida, S.; Musacchio, A.; Knapp, S. Crystal Structure of Human Aurora B in Complex with INCENP and VX-680. *J. Med. Chem.* **2012**, *55*, 7841–7848. [[CrossRef](#)]
39. Degorce, S.L.; Boyd, S.; Curwen, J.O.; Ducray, R.; Halsall, C.T.; Jones, C.D.; Lach, F.; Lenz, E.M.; Pass, M.; Pass, S.; et al. Discovery of a Potent, Selective, Orally Bioavailable, and Efficacious Novel 2-(Pyrazol-4-ylamino)-pyrimidine Inhibitor of the Insulin-like Growth Factor-1 Receptor (IGF-1R). *J. Med. Chem.* **2016**, *59*, 4859–4866. [[CrossRef](#)]
40. Zhang, Q.; Sang, F.; Qian, J.; Lyu, S.; Wang, W.; Wang, Y.; Li, Q.; Du, L. Identification of novel potential PI3K α inhibitors for cancer therapy. *J. Biomol. Struct. Dyn.* **2020**, *39*, 3721–3732. [[CrossRef](#)]

41. Bai, L.; Zhou, H.; Xu, R.; Zhao, Y.; Chinnaswamy, K.; McEachern, D.; Chen, J.; Yang, C.-Y.; Liu, Z.; Wang, M.; et al. A Potent and Selective Small-Molecule Degradator of STAT3 Achieves Complete Tumor Regression In Vivo. *Cancer Cell* **2019**, *36*, 498–511. [e17](#). [[CrossRef](#)] [[PubMed](#)]
42. Sardar, A.; Abid, O.-U.; Daud, S.; Fakhar-E-Alam, M.; Siddique, M.H.; Ashraf, M.; Shahid, W.; Ejaz, S.A.; Atif, M.; Ahmad, S.; et al. Design, synthesis, in vitro and in silico studies of naproxen derivatives as dual lipoxygenase and α -glucosidase inhibitors. *J. Saudi Chem. Soc.* **2022**, *26*, 101468. [[CrossRef](#)]
43. Alderawy MQ, A.; Alrubaie LA, R.; Sheri, F.H. Synthesis, Characterization of Ibuprofen N-Acyl-1, 3, 4-Oxadiazole Derivatives and Anti-cancer Activity against MCF-7 Cell Line. *Syst. Rev. Pharm.* **2020**, *11*, 681–689. [[CrossRef](#)]
44. Shaikh, M.H.; Subhedar, D.D.; Nawale, L.; Sarkar, D.; Khan, F.A.K.; Sangshetti, J.N.; Shingate, B.B. 1,2,3-Triazole derivatives as antitubercular agents: Synthesis, biological evaluation and molecular docking study. *MedChemComm* **2015**, *6*, 1104–1116. [[CrossRef](#)]
45. Abutaha, N.; Al-Mekhlafi, F.A.; Almutairi, B.O.; Wadaan, M.A. S-phase cell cycle arrest, and apoptotic potential of Echium arabicum phenolic fraction in hepatocellular carcinoma HepG2 cells. *J. King Saud Univ.—Sci.* **2021**, *34*, 101735. [[CrossRef](#)]
46. Win, T.S.; Malik, A.A.; Prachayasittikul, V.S.; Wikberg, J.E.; Nantasenamat, C.; Shoombuatong, W. HemoPred: A web server for predicting the hemolytic activity of peptides. *Futur. Med. Chem.* **2017**, *9*, 275–291. [[CrossRef](#)]
47. Le, P.T.; Cheng, H.; Ninkovic, S.; Plewe, M.; Huang, X.; Wang, H.; Bagrodia, S.; Sun, S.; Knighton, D.R.; Rogers, C.M.L.; et al. Design and synthesis of a novel pyrrolidinyl pyrido pyrimidinone derivative as a potent inhibitor of PI3K α and mTOR. *Bioorganic Med. Chem. Lett.* **2012**, *22*, 5098–5103. [[CrossRef](#)]
48. Thomsen, R.; Christensen, M.H. MolDock: A New Technique for High-Accuracy Molecular Docking. *J. Med. Chem.* **2006**, *49*, 3315–3321. [[CrossRef](#)]

Disclaimer/Publisher's Note: The statements, opinions and data contained in all publications are solely those of the individual author(s) and contributor(s) and not of MDPI and/or the editor(s). MDPI and/or the editor(s) disclaim responsibility for any injury to people or property resulting from any ideas, methods, instructions or products referred to in the content.